JBC RESEARCH ARTICLE

Expanded substrate specificity supported by P1′ and P2′ residues enables bacterial dipeptidyl-peptidase 7 to degrade bioactive peptides

Received for publication, October 1, 2021, and in revised form, January 6, 2022 Published, Papers in Press, January 13, 2022,
https://doi.org/10.1016/j.jbc.2022.101585

Yuko Ohara-Nemoto[1], Yu Shimoyama[2], Toshio Ono[1], Mohammad Tanvir Sarwar[1], Manami Nakasato[3], Minoru Sasaki[2], and Takayuki K. Nemoto[1,*]

From the [1]Department of Oral Molecular Biology, Course of Medical and Dental Sciences, Nagasaki University Graduate School of Biomedical Sciences, Nagasaki, Japan; [2]Division of Molecular Microbiology, Department of Microbiology, Iwate Medical University, Yahaba-cho, Iwate, Japan; [3]Division of Periodontology, Department of Conservative Dentistry, Iwate Medical University School of Dentistry, Morioka, Iwate, Japan

Edited by George DeMartino

Dipeptide production from extracellular proteins is crucial for *Porphyromonas gingivalis*, a pathogen related to chronic periodontitis, because its energy production is entirely dependent on the metabolism of amino acids predominantly incorporated as dipeptides. These dipeptides are produced by periplasmic dipeptidyl-peptidase (DPP)4, DPP5, DPP7, and DPP11. Although the substrate specificities of these four DPPs cover most amino acids at the penultimate position from the N terminus (P1), no DPP is known to cleave penultimate Gly, Ser, Thr, or His. Here, we report an expanded substrate preference of bacterial DPP7 that covers those residues. MALDI-TOF mass spectrometry analysis demonstrated that DPP7 efficiently degraded incretins and other gastrointestinal peptides, which were successively cleaved at every second residue, including Ala, Gly, Ser, and Gln, as well as authentic hydrophobic residues. Intravenous injection of DPP7 into mice orally administered glucose caused declines in plasma glucagon-like peptide-1 and insulin, accompanied by increased blood glucose levels. A newly developed coupled enzyme reaction system that uses synthetic fluorogenic peptides revealed that the P1′ and P2′ residues of substrates significantly elevated k_{cat} values, providing an expanded substrate preference. This activity enhancement was most effective toward the substrates with nonfavorable but nonrepulsive P1 residues in DPP7. Enhancement of k_{cat} by prime-side residues was also observed in DPP11 but not DPP4 and DPP5. Based on this expanded substrate specificity, we demonstrate that a combination of DPPs enables proteolytic liberation of all types of N-terminal dipeptides and ensures *P. gingivalis* growth and pathogenicity.

Periodontal diseases are commonly seen in developed countries and a leading cause of tooth loss in adults. *Porphyromonas gingivalis*, a Gram-negative anaerobic and asaccharolytic rod, is one of the potent causatives of severe periodontal diseases and strikingly associated with clinical measures (1, 2). In addition to the association of tooth loss with decrement in quality of life in elderly individuals, *P. gingivalis* is closely related to systemic diseases, such as type 2 diabetes mellitus (3–5), atherosclerotic cardiovascular disorder (6, 7), decreased kidney function (8), rheumatoid arthritis (9), and Alzheimer's disease (10). Regardless of the recent emphasis on periodontal and systemic diseases, molecular mechanisms linking oral and systemic disorders remain to be elucidated. One proposal with broad support states that in type 2 diabetes cases, lipopolysaccharide from periodontopathic bacteria chronically increases the level of tumor necrosis factor alpha, leading to insulin resistance (11). In addition, we previously demonstrated more direct involvement, as *P. gingivalis* dipeptidyl-peptidase (DPP)4 was shown to degrade incretin peptides the same as a mammalian entity, resulting in elevation and prolongation of postprandial hyperglycemia in a mouse model (12).

P. gingivalis growth is not supported by carbohydrates but rather by proteinaceous nutrients, since the bacterium exclusively utilizes amino acids as its carbon and energy sources. Previous studies suggested that amino acids are mostly incorporated as dipeptides into bacterial cells (13–15). In accord with these findings, we recently reported that the bacterium predominantly takes up dipeptides rather than single amino acids and tripeptides or oligopeptides. Dipeptides are mainly transported across the plasma membrane *via* the proton-dependent oligopeptide transporter. Hence, the growth of *P. gingivalis* was markedly retarded in the proton-dependent oligopeptide transporter–deficient mutant but not in amino acid transporter *sstT* and tripeptide transporter *opt* mutants (16). Dipeptide-dominant incorporation closely corresponds to the existence of a series of DPPs and exopeptidases in periplasmic space, which liberate various dipeptides from the N terminus of polypeptides. In contrast, aminopeptidase activities are scarce in the bacterium (17), which is compatible with the subsidiary role of the amino acid transporter SstT in bacterial growth.

* For correspondence: Takayuki K. Nemoto, tnemoto@nagasaki-u.ac.jp.
Present address for Mohammad Tanvir Sarwar: Department of Applied Nutrition and Food Technology, Faculty of Biological Sciences, Islamic University, Kushtia 7003, Bangladesh.

DPP is an exopeptidase that releases a dipeptide from the nonblocked N terminus of peptides and does not hydrolyze the peptide bond between the penultimate residue from the N terminus (P1 position) and third Pro. Two other exopeptidases, that is, acylpeptidyl oligopeptidase (18) and prolyl tripeptidyl-peptidase A (19), are known to liberate acylated N-terminal dipeptides or tripeptides and Xaa-Yaa-Pro, respectively, and manage these inappropriate substrates and then provide substrates accessible to DPPs (20).

DPPs are categorized by substrate specificity, which is primarily defined by the amino acid residue at the P1 position. DPP4 (S9.013 in the MEROPS peptidase database) (21) is specific for P1 Pro and accepts Ala to some extent (22–24), whereas DPP5 (S9.075) is most preferential for Ala and hydrophobic residues (25, 26). Furthermore, DPP7 (S46.001) prefers hydrophobic P1 residues (27), and DPP11 (S46.002) is specific for Asp and Glu (28). Although information regarding amino acid preference other than the P1 residue is limited, it has been shown that the hydrophobic residue at the P2 position enhances the activities of DPP7 and DPP11 (29) but not of DPP5 (26).

All four DPPs are serine peptidases harboring the essential Ser, Asp, and His, whose locations in the amino acid sequences are distinct between the S9 and S46 family members. For instance, the catalytic triads in *P. gingivalis* DPP4 (Ser^{593}, Asp^{669}, and His^{700}) and DPP5 (Ser^{542}, Asp^{672}, and His^{659}) are located at the C-terminal domain, whereas those in DPP7 (His^{89}, Asp^{196}, and Ser^{648}) and DPP11 (His^{85}, Asp^{198}, and Ser^{655}) are distributed in the entire amino acid sequences.

Even though the P1 specificities of the four DPPs seem to cover most amino acid residues, hydrolysis analysis using synthetic dipeptidyl-4-methycoumaryl-7-amide (MCA) showed poor cleavage of several substrates, including Thr-Ser-MCA, Gly-Gly-MCA, and Ala-Asn-MCA, by *P. gingivalis* cells (26). In accord with these observations, to date, no DPP has been reported to efficiently hydrolyze dipeptidyl-MCA or *p*-nitroanilide with P1-position Ser, Gly, Thr, Asn, and His. Therefore, we wonder whether *P. gingivalis* endures this disadvantage or possesses an unidentified exopeptidase(s) or mechanism to effectuate complete dipeptide production.

Human DPP4/CD26 is a multifunctional molecule involved in T-cell activation as well as degradation of a broad range of bioactive proteins and peptides. For example, DPP4 liberates His/Thr-Ala from the N terminus of incretin, that is, glucagon-like peptide-1 (GLP-1) and gastric inhibitory polypeptide (GIP), resulting in their inactivation (30). Since active incretins induce insulin secretion from pancreatic β cells, DPP4 inhibitors are used to treat patients suffering from type 2 diabetes mellitus to prolong the half-life of incretins (31). Our findings that DPP4 of *P. gingivalis* and other periodontopathic bacteria degrade incretins and modulate host blood glucose levels (12) led us to speculate a connection between bacterial DPPs and degradation of bioactive peptides causing derangement of homeostasis or physiological regulatory systems in humans.

In the present study, mass spectrometry (MS) analyses revealed that *P. gingivalis* DPP7 has more potent hydrolyzing activity toward incretins and other gastrointestinal peptides than DPP4. To elucidate the mechanism related to this enhanced activity, we investigated the association of amino acid residues at the P2, P1′, and P2′ positions with the activities of the four DPPs by use of a newly developed two-step reaction using synthetic tri-peptidyl-MCA and tetra-peptidyl-MCA with a second exopeptidase.

Results

Degradation of incretins by P. gingivalis

Degradation of bioactive peptides could correlate with severe periodontal diseases and systemic disorders. We first investigated whether DPP4 is the sole entity responsible for degradation of incretins in *P. gingivalis*. If so, it was considered that the peak level of active GLP-1 (amino acids: 7–37) in MALDI-TOF MS analysis would not change after incubation with the *dpp4*-deficient strain NDP200. Although the peak remained intact for 30 min at 37 °C (12), prolonged incubation for 2 h produced the peak of GLP-1 (amino acids: 9–37) (Fig. 1*A*), indicating commitment of another DPP. We speculated an involvement of DPP5 because it efficiently hydrolyzes Lys-Ala-MCA (26). However, the degradation product was still observed in NDP110 (Δ*dpp4*–Δ*dpp5*). Unexpectedly, the N-terminal-truncated peak disappeared in both NDP211 (Δ*dpp4*–Δ*dpp5*–Δ*dpp7*) and NDP210 (Δ*dpp4*–Δ*dpp7*), suggesting an involvement of DPP7 in the truncation. Finally, we found that single deletion of *dpp7* of NDP400 was sufficient for maintaining the active form of GLP-1 (amino acids: 7–37) under our conditions. These results indicated degradation of GLP-1 by DPP7, which seemed more efficient than DPP4.

We compared the hydrolysis potential of recombinant forms of *P. gingivalis* DPPs (100 ng) for GLP-1. DPP4 degraded GLP-1 (amino acids: 7–37) solely into Glu^{9}–Gly^{37} as previously reported (12). In accord with the results obtained with mutant strains, nearly no cleavage of Ala^{8}–Glu^{9} with DPP5 was observed (Fig. 1*B*), whereas DPP11 did not degrade the peptide (data not shown). In contrast, DPP7 completely degraded GLP-1 (amino acids: 7–37), mainly into Glu^{21}–Gly^{37}. Time-course analysis with the substrate–enzyme molar ratio (160:1) was conducted, and DPP7 was found to completely degrade GLP-1 within 15 min, whereas 15% of the intact form remained with DPP4. DPP7 achieved sequential dipeptide truncation until Ala^{25}–Gly^{37}, accompanying three dominant forms (Gln^{9}–Gly^{37}, Thr^{13}–Gly^{37}, and Glu^{21}–Gly^{37}). This hydrolysis pattern of DPP7 was likely caused by rapid cleavages between Ala^{8}–Glu^{9}, Phe^{12}–Thr^{13}, and Leu^{20}–Glu^{21}, and bottleneck reactions at Gly^{10}–Thr^{11}, Ser^{14}–Asp^{15}, and Gly^{22}–Gln^{23} (Fig. 1, *C* and *D*). Thus, these results demonstrated an expanded repertoire of DPP7 toward P1 Gly (hydrophobicity index [HI] = 0) and Ser (HI = −5) (32) (Fig. 1*D*). Although GLP-1 was thoroughly degraded by recombinant DPP7 (100 ng) but not by *P. gingivalis* cells (compare Figs. 1*A* and 2, *B* and *C*), this difference should be caused by the limited amounts of cell-associated DPP7 against the recombinant molecule.

Degradation of the second incretin peptide GIP (52–93) was also examined with increasing amounts of *P. gingivalis* DPPs.

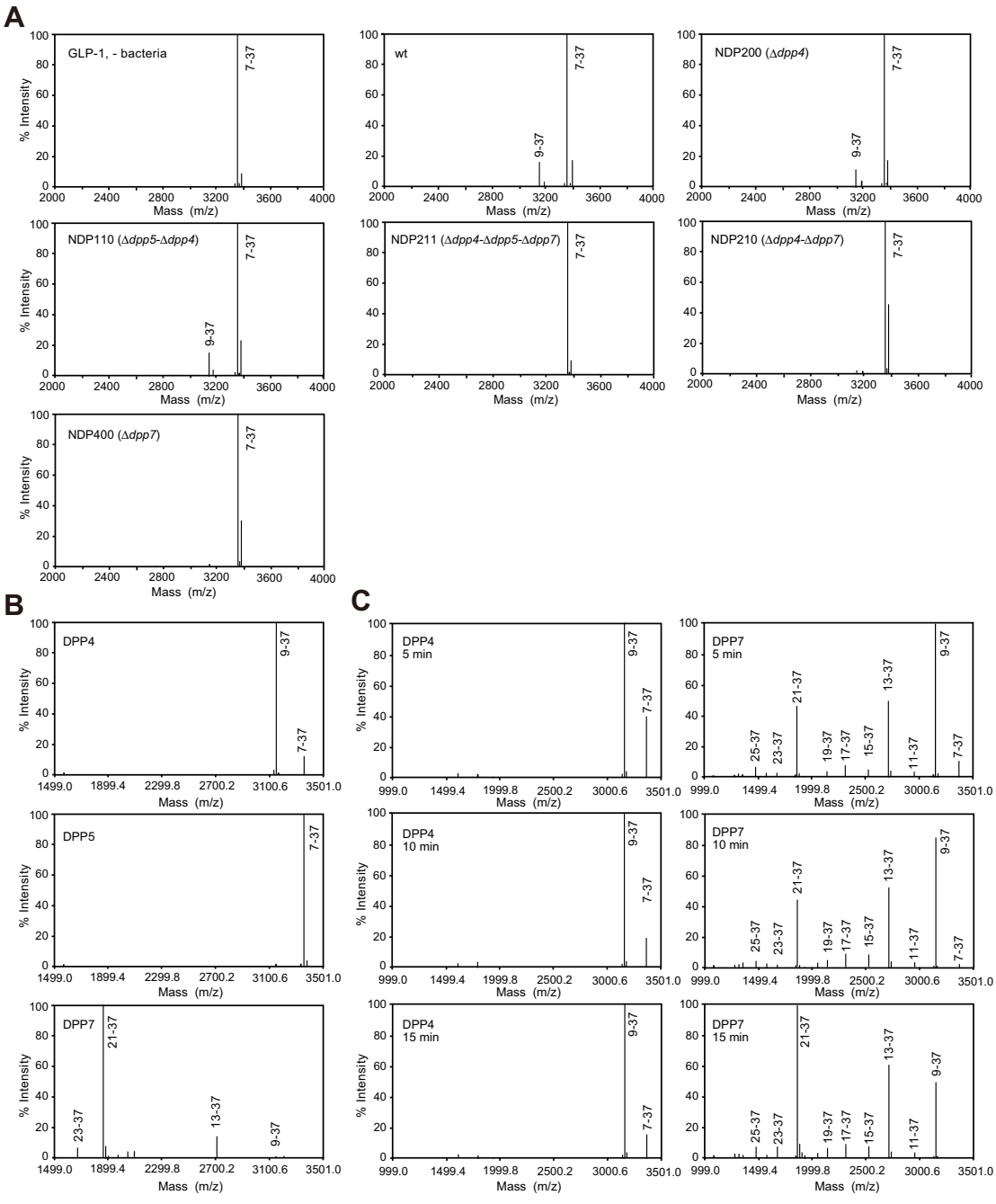

D

GLP-1 peptide	mass
$H^{7}AEGTFTSDVSSYLEGQAAKEFIAWLVKGRG^{37}$	3355.71
$E^{9}GTFTSDVSSYLEGQAAKEFIAWLVKGRG^{37}$	3147.49
$T^{11}FTSDVSSYLEGQAAKEFIAWLVKGRG^{37}$	2961.32
$T^{13}SDVSSYLEGQAAKEFIAWLVKGRG^{37}$	2713.04
$D^{15}VSSYLEGQAAKEFIAWLVKGRG^{37}$	2524.86
$S^{17}SYLEGQAAKEFIAWLVKGRG^{37}$	2310.64
$Y^{19}LEGQAAKEFIAWLVKGRG^{37}$	2136.48
$E^{21}GQAAKEFIAWLVKGRG^{37}$	1860.15
$Q^{23}AAKEFIAWLVKGRG^{37}$	1673.98
$A^{25}KEFIAWLVKGRG^{37}$	1474.77

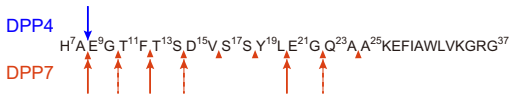

Figure 1. Degradation of GLP-1 (amino acids: 7–37) by *Porphyromonas gingivalis* strains and recombinant DPPs. *A*, GLP-1 (amino acids: 7–37) (20 μM) was incubated at 37 °C for 2 h without (−bacteria) or with *P. gingivalis* ATCC 33277 (wt), NDP200 (Δ*dpp4*), NDP110 (Δ*dpp4*—Δ*dpp5*), NDP211 (Δ*dpp4*–Δ*dpp5*–Δ*dpp7*), NDP210 (Δ*dpp4*–Δ*dpp7*), and NDP400 (Δ*dpp7*) and then analyzed by MALDI-TOF mass spectrometry as described in the "Experimental procedures" section. The reaction was performed in the presence of 0.5 mM TLCK and 30 μM E-64 to suppress gingipain activities. *B*, GLP-1 (amino acids: 7–37) (20 μM) was incubated for 30 min with 100 ng of DPP4, DPP5, and DPP7 (molar ratio of substrate:enzyme = 160:1. *C*, GLP-1 (amino acids: 7–37) (20 μM) was incubated with 100 ng of DPP4 and DPP7 for 5, 10, and 15 min. *D*, amino acid sequences and molecular masses are presented. DPP4 cleavage site is shown by *arrow* (*blue*). Sites of cleavage by DPP7 are indicated by *arrowheads* (*red*), among which fast and slowly cleaved sites are shown by *solid* and *dashed arrows*, respectively. ATCC, American Type Culture Collection; DPP, dipeptidyl-peptidase; E-64, [(2*S*, 3*S*)-3-carboxyoxirane-2-carbonyl]-L-leucine (4-guanidinobutyl) amide hemihydrate; GLP-1, glucagon-like peptide-1; TLCK, tosyl-L-lysyl-chloromethane hydrochloride.

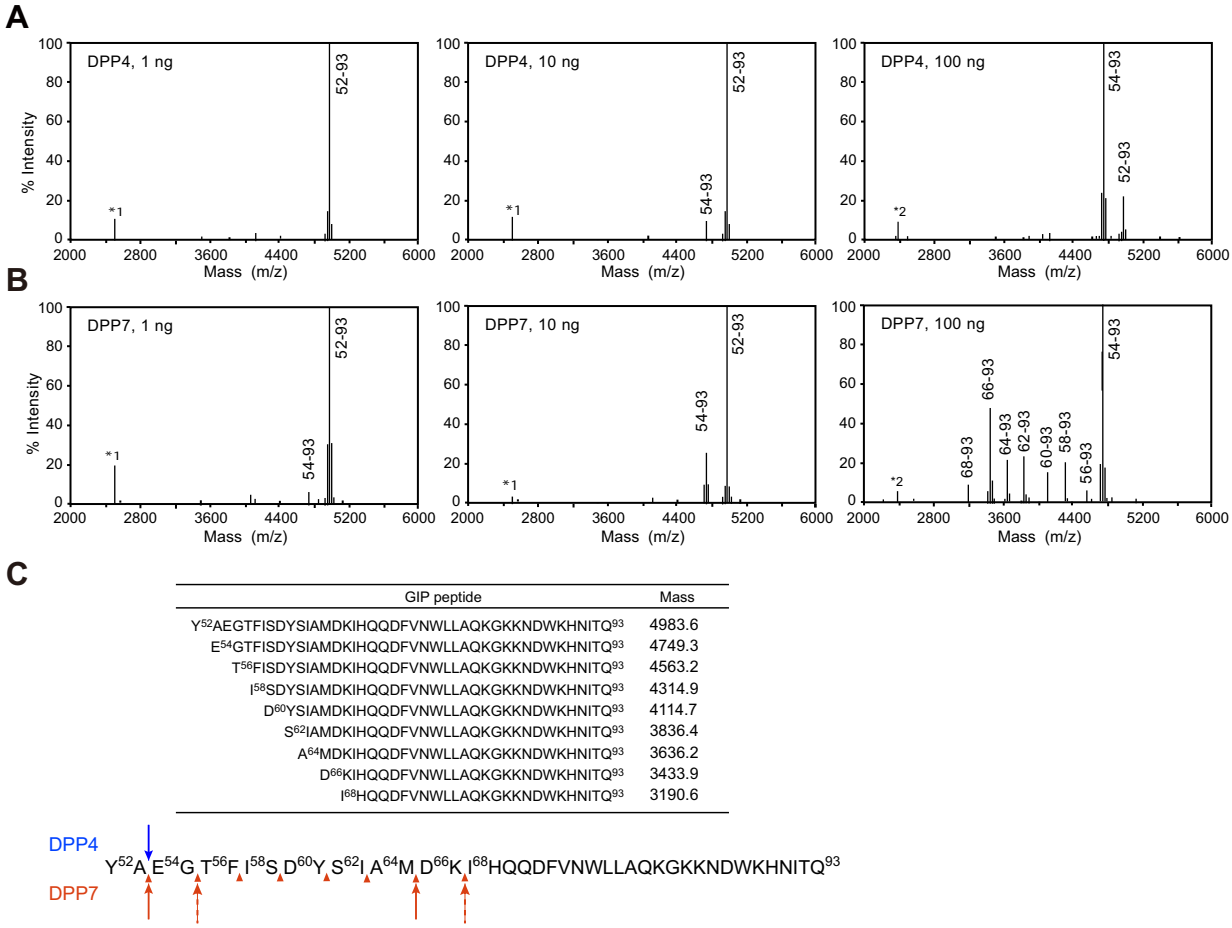

Figure 2. Degradation of GIP (amino acids 52–93) by DPP4 and DPP7. GIP (amino acids: 52–93) (20 μM) was incubated with 1 (molar ratio, 16,000:1), 10 (1600:1), or 100 ng (160:1) of (*A*) DPP4 or (*B*) DPP7 at 37 °C for 5 min. *[1] and *[2] indicate unidentified peaks. *C*, amino acid sequences and molecular masses of GIP (amino acids: 52–93) and its degradation products are presented. DPP4 cleavage site is shown by an *arrow* (*blue*). Cleavage sites of DPP7 are indicated by *arrowheads* (*red*), among which fast and slowly cleaved sites are shown by *solid and dashed arrows*, respectively. DPP, dipeptidyl-peptidase; GIP, gastric inhibitory polypeptide.

The N-terminal sequence (Y^{52}AEGTF*ISDYSIAM*^{65}—) of GIP (52–93) is distinct from that of GLP-1 (amino acids: 7–37) (H^{7}AEGTF*TSDVSSYL*^{20}—) at several positions (indicated by italics). Five minutes after starting incubation, DPP5 and DPP11 did not degrade GIP (52–93) even with 100 ng (data not shown), whereas GIP (52–93) was converted to GIP (54–93) by DPP4 in a dose-dependent manner (Fig. 2). DPP7 again liberated the N-terminal dipeptide with 10 ng, faster than DPP4, and with 100 ng resulted in successive cleavages. The peaks of Glu^{54}-Gln^{93} and Asp^{66}-Gln^{93} were relatively high, suggesting more rapid cleavage between Ala^{53}-Glu^{53} and Met^{65}-Asp^{66} and bottleneck reactions at Gly^{55}-Thr^{56} and Lys^{67}-Ile^{68}. Degradation products of Ile^{58}-Gln^{93}, Ser^{62}-Gln^{93}, and Ala^{64}-Gln^{93} were shown as moderate peaks. Taken together, these results demonstrated the expanded substrate specificity of *P. gingivalis* DPP7 to Gly (HI = 0), Ser (HI = −5), and even Lys (HI = −23), in addition to authentic hydrophobic residues, such as Phe (100), Ile (99), Met (74), Tyr (63), and Ala (41) (Fig. 2*C*), and that the degradation rates against former residues seemed to be slower than those for the latter.

Analysis of *in vitro* degradation of incretins suggested that DPP7 may have an effect on blood glucose levels in patients infected with *P. gingivalis* and suffering from a severe form of periodontal diseases. We thus performed a glucose tolerance test in mice according to the previous report (12). Sterilized *P. gingivalis* DPP7 (1 U 100 μl^{-1} PBS, pH 7.3) or PBS (100 μl) was injected into the tail vein of mice after fasting for 12 h. Following oral administration of glucose, blood glucose levels were measured for 2 h. As shown in Figure 3, more significant hyperglycemia was observed with DPP7 than PBS, and higher glucose levels continued throughout the testing period. At 15 min after glucose administration, increased glucose level and decreased plasma concentrations of active GLP-1 and insulin were noted. These results showed that *P. gingivalis* DPP7 could function *in vivo* to modulate blood glucose levels, similar to periodontopathic bacterial and mammalian DPP4.

Degradation of bioactive peptides by DPP7

Degradation of incretins indicates an expanded substrate specificity of *P. gingivalis* DPP7 and its possible functions to modulate physiological regulation systems. To further characterize the potential of DPP7, we examined the hydrolysis activities of DPP4 and DPP7 for several bioactive peptides

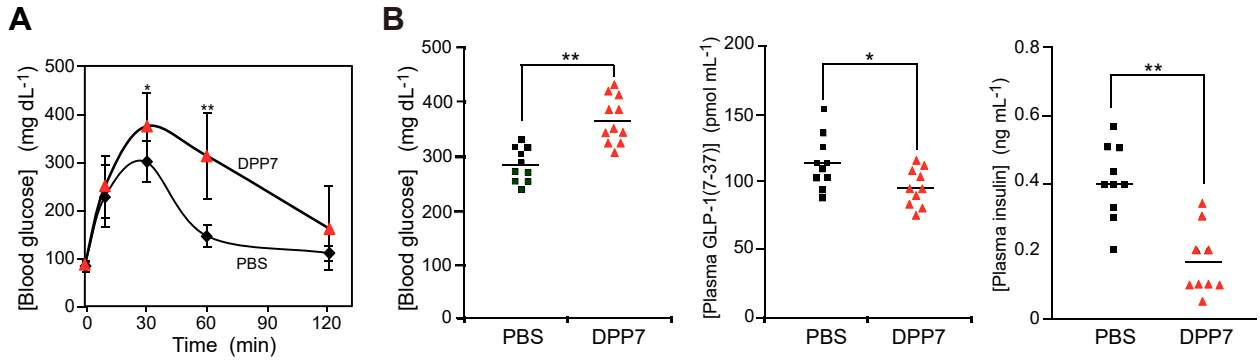

Figure 3. Glucose tolerance test using mice injected with recombinant DPP7. *A*, 2 min after intravenous injection of DPP7 (1 U 100 μl^{-1} PBS) or PBS (100 μl) to mice, a glucose solution (3 mg/g body weight) was orally administrated. Blood glucose concentrations (mean ± SD, n = 4) were determined up to 2 h after glucose administration. Representative results from three independent experiments are shown. *B*, concentrations (mean ± SD) of blood glucose, plasma GLP-1, and insulin at 15 min after glucose administration were determined. *$p < 0.05$, **$p < 0.01$ (*versus* PBS; Student's *t* test). DPP, dipeptidyl-peptidase; GLP-1, glucagon-like peptide-1.

using MS and compared their half-lives (Table 1 and Fig. S1). Those were human glucagon (29 amino acids) and its C-terminally elongated form oxyntomodulin (37 amino acids) as additional gastrointestinal hormones, substance-P (11 amino acids) as a neuropeptide, and chemokine (C–C motif) ligand 3 (CCL3) (70 amino acids) and chemokine (C–X–C motif) ligand 6 (CXCL6) (70 amino acids) as chemokines, which were previously examined as substrates for human DPP4 (23). In addition, bovine insulin (21 amino acids of A chain and 30 amino acids of B chain) was examined. *P. gingivalis* DPP4 (0.5 μg ml^{-1}, substrate:enzyme molar ratio = 800: 1) released the N-terminal dipeptides from GLP-1 and GIP with $t_{1/2}$ of 16 and 3 min, respectively, whereas it did not hydrolyze insulin and scarcely hydrolyzed glucagon and oxyntomodulin. DPP4 liberated the N-terminal tetrapeptide from substance-P by cleavage at the Pro^2-Lys^3 and Pro^4-Gln^5 bonds with $t_{1/2}$ of 24 min. Accordingly, *P. gingivalis* DPP4 solely degraded at Pro^2/Ala^2-Xaa^3 bonds as established in previous studies (12, 24).

In accord with the results of Figures 1 and 2, faster degradation of GLP-1 and GIP by DPP7 as compared with DPP4 was observed (Table 1 and Fig. S1). Interestingly, DPP7 at 8000:1 slowly cleaved the insulin B chain, whereas that at 800:1 cleaved both the A and B chains with a $t_{1/2}$ of 18 and 5 min, respectively. The cleavage sites were shown to be located between Ile-Val, Glu-Gln, Val-Asn, Gln-His, and Leu-Cys. The slower cleavage of insulin as compared with incretins was presumably because of its rigid structure composed of three disulfide bonds. Glucagon and oxyntomodulin were efficiently cleaved at 8000:1 with a $t_{1/2}$ of 25 to 27 min after P1 Ser, Gly, Phe, Tyr, Lys, and Leu. In contrast, DPP7 truncated CXCL6 very slowly at a ratio of 800:1, whereas substance-P, possessing P1 Pro and CCL3 with a disulfide bond (C–C motif) near its N terminus, was not cleaved. These results indicated that DPP7 could degrade several bioactive peptides even with nonhydrophobic P1 residues Gln (HI = −10) and Glu (HI = −31).

Hydrolyzing activity of DPPs toward Xaa-Ala-MCA

The present results showing the degradation of bioactive peptides strongly suggested that residues other than P1 position affect the activity of DPP7 and that this effect seemed distinct among *P. gingivalis* DPPs. Then, we initially examined the effect of P2 using dipeptidyl-MCA substrates (Lys-Ala, Gly-Ala, His-Ala, and Tyr-Ala) harboring P1 Ala, as in GLP-1 and GIP. Lys-Ala-MCA has been one of established substrates for DPP5 (26). As shown in Figure 4, DPP11 did not show any hydrolysis for these substrates. Lys-Ala-MCA was most efficiently hydrolyzed by DPP4, followed by DPP5, whereas that was scarce with DPP7. Gly-Ala-MCA was more slowly hydrolyzed than Lys-Ala-MCA by the three DPPs, whereas DPP5 showed considerable hydrolysis. As compared with the two substrates noted previously, hydrolysis of His-Ala-MCA was least among the four substrates and comparable to that of the three DPPs. Furthermore, hydrolysis of Tyr-Ala-MCA was moderate among the substrates, and DPP7 showed the highest activity. These results indicate that while the P2 residue affects DPP activities, degradation profiles against His-Ala-MCA and Tyr-Ala-MCA do not explain lack of degradation of GLP-1 and GIP by DPP5 or efficient degradation of GLP-1 by DPP7.

Commitment of P1′ and P2′ residues toward DPP7 activity

To evaluate the effects of P1′ and P2′ residues, we compared DPP activities toward His-Ala-MCA and three additional substrates, HAEG-MCA, HAEF-MCA, and HAEGTF-MCA (amino acids identical to N-terminal sequences of GLP-1 [amino acids: 7–37] are underlined). In HAEF-MCA, the fourth Gly (HI = 0) was replaced by Phe (100) because of the hydrophobic preference of DPP7. Although His-Ala-MCA was cleaved to a similar extent by the three DPPs (Figs. 4 and 5*A*), HAEG-MCA, HAEF-MCA, and HAEGTF-MCA were not hydrolyzed by DPP4 because DPP4 cannot degrade Glu-Gly/Phe-MCA after liberation of His-Ala. Although DPP5 degrades His-Ala-MCA and prefers P1 Phe, HAEF-MCA was not hydrolyzed, indicating the inefficiency of two successive hydrolyses of the substrate under these conditions. In contrast, though DPP7 did not cleave HAEG-MCA because of unfavorable Gly, hydrolysis of HAEF-MCA was observed and found to be threefold higher than that of His-Ala-MCA. Moreover, in contrast to no hydrolysis of

Table 1
Degradation of bioactive peptides and proteins by DPP4 and DPP7

Peptidase	Substrate category	Name	Molar ratio (substrate:enzyme)	$t_{1/2}$ (min) and others	N-terminal sequence and cleavage site
P. gingivalis DPP4	Gastrointestinal peptide	GLP-1 (7–37)	800:1	16	HA|EGTFTSDVSSYLEG—
		GIP (52–93)	800:1	3	YA|EGTFISDYSIAMDK—
		Insulin (A, 1–21; B, 1–30)[a]	800:1	Not cleaved	GIVEQCCASVCSLYQLENYCN FVNQHLCGSHLVEALYLVCGERGFFYTPKA
		Glucagon (1–29)	800:1	Scarcely cleaved	HS|QGTFTSDYSKYLDSRRAQ—
		Oxyntomodulin (1–37)	800:1	Not cleaved	HSQGTFTSDYSKYLDSRRAQ—
	Neuropeptide	Substance-P (1–11)	800:1	24	RP|KP|QQFFGLM-NH_2
	Chemokine	CCL3 (1–70)	800:1	Not cleaved	ASLAADTPTACCFSY—
		CXCL6 (1–70)[b]	800:1	Not cleaved	VLTELRCTCLRVTLR—
P. gingivalis DPP7	Gastrointestinal peptide	GLP-1 (7–37)	8000:1	31	HA|EGTFTSDVSSYLEG—
		GIP (52–93)	8000:1	23	YA|EG|TF|IS|DY|SIAMDK—
		Insulin (A, 1–21; B, 1–30)[a]	8000:1	A: Scarcely cleaved B: 70[c]	GI|VEQCCASVCSLYQLENYCN FV|NQ|HLCGSHLVEALYLVCGERGFFYTPKA
			800:1	A: 18 B: 5	GI|VE|QCCASVCSLYQLENYCN FV|NQ|HL|CGSHLVEALYLVCGERGFFYTPKA
		Glucagon (1–29)	8000:1	27	HS|QG|TF|TS|DY|SK|YL|DSRRAQ—
			800:1	<<5	HS|QG|TF|TS|DY|SK|YL|DS|RRAQ—
		Oxyntomodulin (1–37)	8000:1	25	HS|QG|TF|TS|DY|SKYLDSRRAQ—
			800:1	<<5	HS|QG|TF|TS|DY|SK|YL|DS|RRAQ—
	Neuropeptide	Substance-P (1–11)	800:1	Not cleaved	RPKPQQFFGLM-NH_2
	Chemokine	CCL3 (1–70)	800:1	Not cleaved	ASLAADTPTACCFSY—
		CXCL6 (1–70)[b]	8000:1	Not cleaved	VLTELRCTCLRVTLR—
			800:1	52	VL|TELRCTCLRVTLR—
Human DPP4	Gastrointestinal peptide	GLP-1 (7–37)	180:1[d]	9	HA|EGTFTSDVSSYLEG—
		GIP (52–93)	120:1[d]	8	YA|EGTFISDYSIAMDK—
C. canimorsus DPP7	Coagulation factor	FX heavy chain	5.4:1[e]	Not determined	SV|AQ|AT|SS|SG|EAPDSI—
		FX light chain	5.4:1[e]	Not determined	AN|SFLEEM—

Five micromolar substrates were incubated with *P. gingivalis* DPP4 or DPP7 for 0 to 40 min at 37 °C. $t_{1/2}$ of the intact peptides was determined by MALDI-TOF MS analysis (n = 2) as described in Fig. S1. Cleavage sites are indicated by "|". Noncleaved and bottle neck reaction sites are underlined.
[a] Digested as an intact AB dimer.
[b] Main form of the sample subjected to the analysis because of C-terminal truncation at Lys^{70}-|Lys^{71}-Asn^{72}.
[c] Determined by extrapolation.
[d] Calculated from Keane *et al.* (23).
[e] Calculated from Hack *et al.* (36).

HAEG-MCA, a low level but still substantial hydrolysis of HAEGTF-MCA was found, indicating the three-step successive reactions by DPP7. These results strongly suggest that DPP7 activity is enhanced by C-terminal side (prime-side) residues of the cleavage site.

As a means for quantitative and convenient measurement of the effect of the prime-side residues, we developed a coupled enzyme reaction system using new MCA substrates. In HAED-MCA, cleavage at the Ala^2-Glu^3 bond by the first DPP provides Glu-Asp-MCA, which is then hydrolyzed by DPP11 (Fig. 5*B*). DPP11 (up to 10 μg) did not cleave the substrate, whereas degradation occurred in the presence of 10 ng of DPP7 and 0.1 μg of DPP11 and then reached a plateau with 3 μg of DPP11 (Fig. 5*C*). Hence, hydrolyzing activity at the Ala^2-Glu^3 bond could be quantitatively determined with HAED-MCA in the presence of an excessive amount (3 μg) of DPP11.

The effects of the P1′ and P2′ residues on DPP activities were compared using this method. Hydrolyzing activities of DPP4, DPP5, and DPP7 toward His-Ala-MCA were comparable without and with DPP11 (Fig. 5*D*). Although degradation

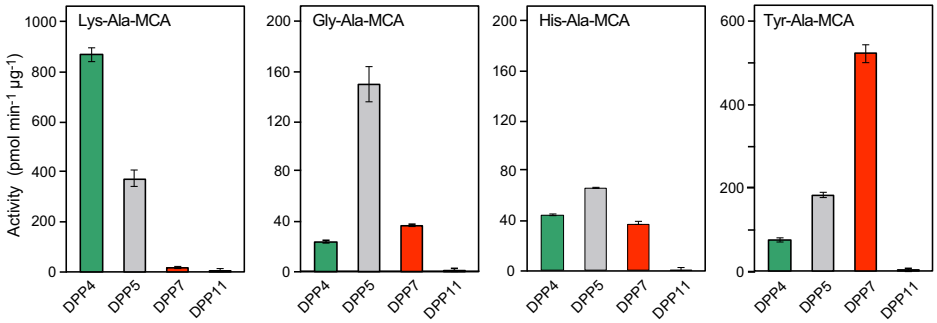

Figure 4. Degradation of dipeptidyl-MCA with P1 Ala by DPPs. Lys-Ala-MCA, Gly-Ala-MCA, His-Ala-MCA, and Tyr-Ala-MCA (20 μM) were incubated with 20 ng of DPP4, DPP5, DPP7, or DPP11. Specific activities (mean ± SD, n = 3) are shown. Data are representative of results from three independent experiments. DPP, dipeptidyl-peptidase; MCA, dipeptidyl-4-methycoumaryl-7-amide.

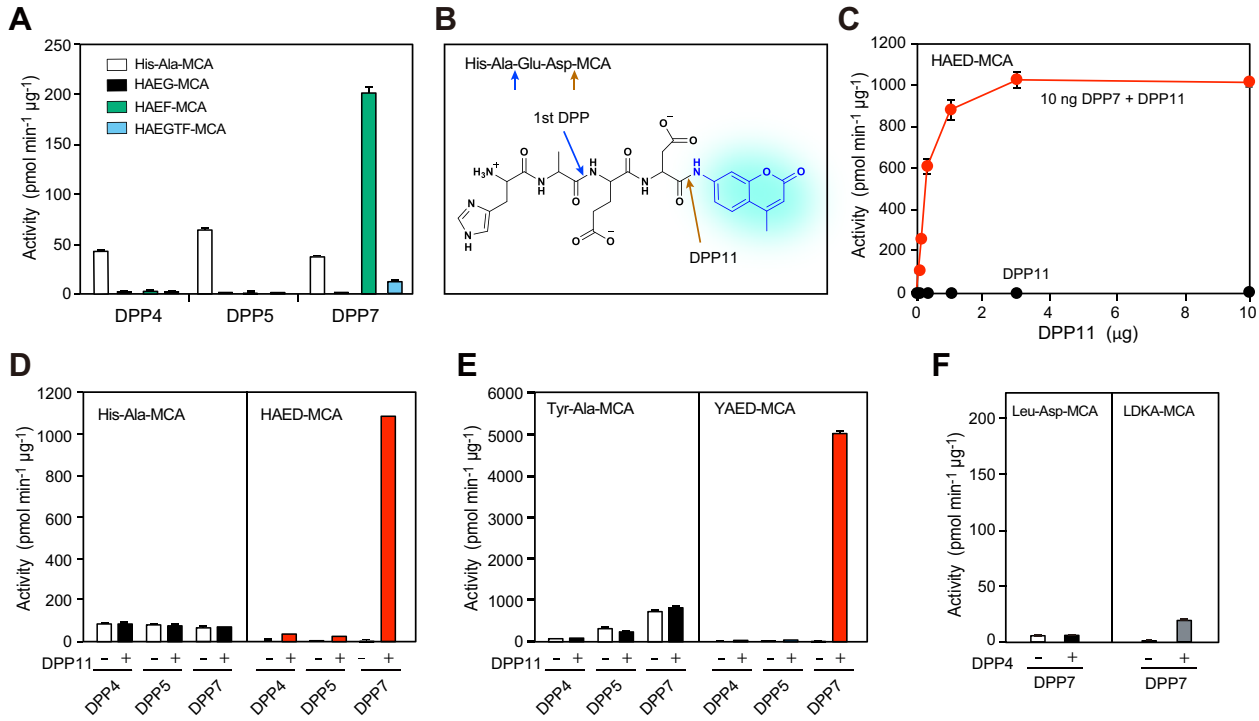

Figure 5. Effects of C-terminal side residues of substrate on DPP activities. *A*, His-Ala-MCA, HAEG-MCA, HAEF-MCA, and HAEGTF-MCA (20 μM) were hydrolyzed by DPP4, DPP5, and DPP7 (0.1 μg). *B*, a chemical formula and cleavage sites of HAED-MCA in the two-step reaction are shown. MCA is indicated in *blue*. *C*, HAED-MCA was hydrolyzed in the absence (*black*) or presence (*red*) of DPP7 (10 ng) together with DPP11 (0–10 μg). *D*, His-Ala-MCA and HAED-MCA were hydrolyzed by DPP4, DPP5, or DPP7 (10 ng) in the absence or the presence of 3 μg of DPP11. *E*, Tyr-Ala-MCA and YAED-MCA were incubated with 10 ng of DPP4, DPP5, and DPP7 in the absence or the presence of 3 μg of DPP11. *F*, Leu-Asp-MCA and LDKA-MCA were hydrolyzed by DPP7 (20 ng) in the absence or the presence of 3 μg of DPP4. Specific activities (mean ± SD, n = 3) are shown. Data are representative of results from at least three independent experiments. DPP, dipeptidyl-peptidase; MCA, dipeptidyl-4-methycoumaryl-7-amide.

of HAED-MCA by both DPP4 and DPP5 was trivial either with or without DPP11, significant elevation (16-fold) of hydrolysis as compared with His-Ala-MCA was achieved with DPP7 in the presence of DPP11. Enhancement of DPP7 activity was also observed with YAED-MCA, in which the first three residues (underlined) are identical to GIP (52–93) (Fig. 5*E*). The activity of DPP7 was 7.4-fold higher than that for Tyr-Ala-MCA, and again no enhancement of hydrolysis toward YAED-MCA was observed with DPP4 or DPP5. These results indicate that DPP7 activity is promoted by prime-side residues. We also found that hydrolysis of HAED-MCA and YAED-MCA by DPP4 and DPP5 in the presence of DPP11 was reduced as compared with that of His-Ala-MCA and Tyr-Ala-MCA, respectively (Fig. 5, *D* and *E*). Presently, it is suspected that an excess amount of DPP11 competitively binds the substrates, causing a decrease in those available for DPP4 and DPP5.

The activity of DPP7 for Tyr-Ala-MCA was 10-fold higher than that for His-Ala-MCA because of the presence of more hydrophobic P2 residue {Tyr [HI = 63] > His [HI = 8]}. On the other hand, when we focused on the increasing activity ratio, hydrolysis of HAED-MCA and YAED-MCA was found to be 16-fold and 7.4-fold higher than that of His-Ala-MCA and Tyr-Ala-MCA, respectively (Fig. 5, *D* and *E*). Therefore, enhancement by the C-terminal dipeptide (Glu-Asp) is more significant for the less preferential substrate harboring P2 His than Tyr. This observation raised another question regarding whether the enhancement is operative even against a substrate with the repulsive P1 residue, such as Asp (HI = −55) and Arg (HI = −14). For example, when hydrolysis of DPP7 against Leu-Asp-MCA and LDKA-MCA in the presence of DPP4 as the second enzyme was compared, a 3.5-fold increase in activity was observed (Fig. 5*F*). This magnitude was substantially lower than that achieved with HAED-MCA (16-fold) and YAED-MCA (7.4-fold), and moreover, the resultant activity remained trivial, possibly because of incompatibility between S1 Gly^{666} of DPP7 and P1 Asp (33). Thus, though activity enhancement of DPP7 mediated by the prime-side residues commonly occurs, it is efficient and meaningful for non-preferential and nonrepulsive alias neutral P1 residues, such as Ala (HI = 41), Gly (HI = 0), and Ser (HI = −5).

Elevation of k_{cat} values of DPP7 by P1′ and P2′ residues

The kinetic parameters of DPP7 were determined using dipeptidyl-MCA, tripeptidyl-MCA, and tetrapeptidyl-MCA (Fig. 6*A* and Table 2). When His-Ala-MCA was compared with the best substrate Phe-Met-MCA, both the K_M and k_{cat} values of the latter were excellent, leading to the high k_{cat}/K_M value. Furthermore, an insertion of two residues between His-Ala and MCA moiety significantly elevated the k_{cat} values by 75-fold for HALD-MCA and 54-fold for HAED-MCA as compared with His-Ala-MCA, whereas the insertion had little effect (1.2–1.6-fold) on K_M.

To specify the commitment of the P1′ and P2′ residues separately, we introduced tripeptidyl-MCA in combination with the second reaction executed by dipeptidase A (DipA)

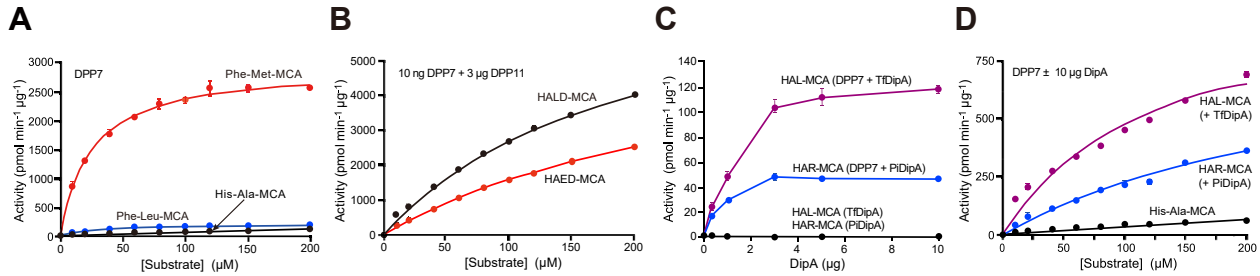

Figure 6. Determination of kinetic constants of DPP7 affected by P1′ and P2′ residues. *A*, Phe-Met-MCA (*red*), Phe-Leu-MCA (*blue*), and His-Ala-MCA (*black*) were incubated with 10, 100, and 100 ng DPP7, respectively. *B*, HALD-MCA (*black*) and HAED-MCA (*red*) were incubated with 10 ng of DPP7 in the presence of 3 µg of DPP11. *C*, HAL-MCA (*purple*) and HAR-MCA (*blue*) (20 µM) were incubated with 10 ng of DPP7 containing 0 to 10 µg of TfDipA and PiDipA, respectively. TfDipA and PiDipA (0.3–10 µg) (*black*) did not cleave the substrates. *D*, His-Ala-MCA (*black*) was incubated with 100 ng of DPP7, whereas HAL-MCA (*purple*) and HAR-MCA (*blue*) were incubated with 10 ng of DPP7 in the presence of TfDipA (10 µg) for HAL-MCA or in the presence of PiDipA (10 µg) for HAR-MCA. Specific activities (mean ± SD, n = 4) are shown. Kinetic parameters were calculated by the GraphPad Prism software and summarized in Table 2. Data are representative of results from three independent experiments. DPP, dipeptidyl-peptidase; MCA, dipeptidyl-4-methycoumaryl-7-amide; PiDipA, dipeptidase A from *Prevotella intermedia*; TfDipA, dipeptidase A from *Tannerella forsythia*.

from *Prevotella intermedia* and *Tannerella forsythia*, which most preferentially recognize Arg-MCA and Leu/Phe-MCA, respectively (34). The hydrolysis of HAR-MCA with DPP7 (10 ng) reached maximal at 3 µg of DipA from *Prevotella intermedia* and that of HAL-MCA reached a plateau with 10 µg of DipA (Fig. 6*C*). Thus, we input 10 µg of Dip A in both reactions. Enhancement by the third residue added to His-Ala-MCA raised k_{cat}, though had little effect on K_M, thus k_{cat}/K_M for HAR-MCA and HAL-MCA was increased by 4.3-fold and 12.7-fold, respectively, from that for His-Ala-MCA (Fig. 6*C* and Table 2). Noticeably, the enhancement magnitude of k_{cat}/K_M from His-Ala-MCA to HAL-MCA and that from HAL-MCA to HALD-MCA was calculated to be 12.8 and 4.7, respectively, which revealed a synergistic contribution of P1′ and P2′ residues to k_{cat}/K_M enhancement.

Elevation of k_{cat} of DPP11 by P1′ and P2′ residues

We previously reported that *P. gingivalis* DPP11 is specific for P1 Asp and Glu but scarcely hydrolyzes His-Asp-MCA or Thr-Asp-MCA (26, 28). In this respect, the hydrophobicity dependence of DPP11 at the P2 position appears to be stronger than that of DPP7 (33), suggesting that DPP11 is unable to hydrolyze all peptides with P1 Asp and Glu. However, the aforementioned findings with the same S46-family DPP7 raised the possibility that DPP11 activity is also elevated by P1′ and P2′ residues. To examine this speculation, we used Leu-Asp-MCA, an established DPP11-specific substrate, Thr-Asp-MCA, a scarcely hydrolyzed substrate in *P. gingivalis* cells, and their elongated substrates, LDKA-MCA and TDKA-MCA. Tetrapeptidyl-MCA was first hydrolyzed by DPP11 (5 ng) and next by DPP4, then reached a maximal level in the presence of 3 µg of DPP4 (Fig. 7). The k_{cat}/K_M value of the DPP11-specific substrate, Leu-Asp-MCA, was 309-fold higher than that of Thr-Asp-MCA, mainly because of markedly higher k_{cat} (Table 2). Insertion of Lys-Ala as the P1′ and P2′ residues to the two substrates had little effect on K_M, whereas that significantly raised k_{cat} values (Fig. 7 and Table 2). Notably, k_{cat} of TDKA-MCA was increased 309-fold from Thr-Asp-MCA, thus k_{cat}/K_M of TDKA-MCA reached 31.4% of Leu-Asp-MCA. Therefore, DPP11 was shown to manage nearly all or all the combinations of P2 residues and P1 Asp and Glu. Accordingly, such expanded substrate specificity achieved by P1′ and P2′ residues is a common phenomenon for S46-family DPP7 and DPP11, and the effect is more significant with nonideal nonrepulsive, that is, neutral substrates.

It should be noted that K_M and k_{cat} values of DPP7 for His-Ala-MCA, HALD-MCA, HAED-MCA, and HAL-MCA and those of DPP11 for TDKA-MCA contain ambiguities as their kinetic fits were determined using only substrate concentrations near or below K_M (Table 2). However, the data compellingly show that there are large increases in k_{cat} when P1′ and P2′ residues are present. These examples make a clear case that primed-side interactions confer expanded P1 substrate specificity on DPP7 and DPP11.

Table 2
Kinetic parameters of DPP7 and DPP11 for peptidyl-MCA

DPP	MCA peptide	K_M (µM)	k_{cat} (s^{-1})	k_{cat}/K_M (s^{-1} $µM^{-1}$)
DPP7	Phe-Met	23.9 ± 1.3	4005 ± 90	168 ± 10
	Phe-Leu	20.6 ± 2.0	466 ± 1	22.7 ± 1.4
	His-Ala	152 ± 22	139 ± 12	0.923 ± 0.065
	HALD	188 ± 30	10,450 ± 1090	55.9 ± 3.4
	HAED	247 ± 19	7520 ± 379	30.5 ± 0.9
	HAL	121 ± 11	1422 ± 67	11.8 ± 0.5
	HAR	336 ± 73	1333 ± 210	4.01 ± 0.30
DPP11	Leu-Asp	14.1 ± 1.0	16,500 ± 600	1170 ± 53
	Thr-Asp	70.4 ± 8.3	265 ± 18	3.79 ± 0.34
	LDKA	14.9 ± 1.2	22,890 ± 510	1547 ± 91
	TDKA	225 ± 59	81,870 ± 17,250	368 ± 21

Kinetic parameters were determined as shown in Figures 6 and 7. Values are means ± SD (n = 4).

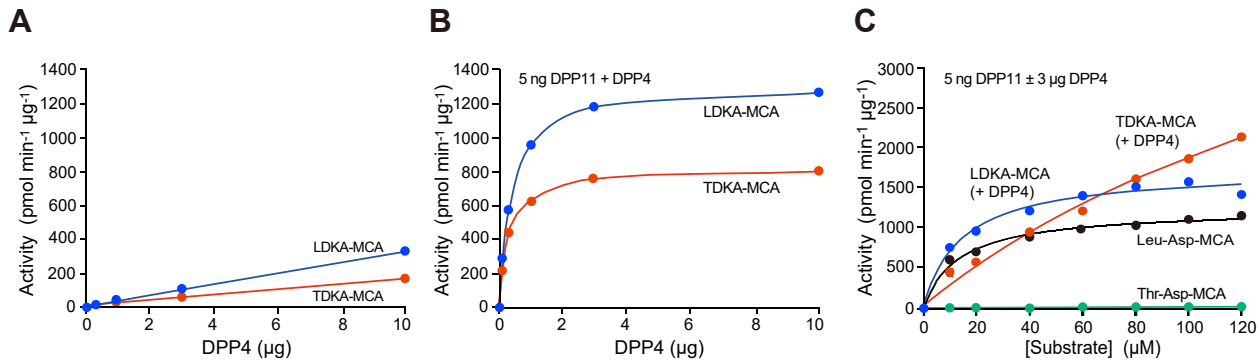

Figure 7. Determination of kinetic constants of DPP11 with tetrapeptidyl-MCA. *A*, LDKA-MCA (*blue*) and TDKA-MCA (*red*) (20 µM) were incubated with DPP4. *B*, LDKA-MCA (*blue*) and TDKA-MCA (*red*) were incubated with 5 ng of DPP11 containing 0 to 10 µg of DPP4. *C*, Leu-Asp-MCA (*black*) and Thr-Asp-MCA (*green*) were incubated with 5 and 100 ng of DPP11, respectively, and LDKA-MCA (*blue*) and TDKA-MCA (*red*) were incubated with 5 ng of DPP11 in the presence of DPP4 (3 µg). Specific activities with subtraction of the hydrolysis by 3 µg of DPP4 (mean ± SD, n = 4) are shown. Kinetic parameters were calculated and summarized in Table 2. Data are representative of results from three independent experiments. DPP, dipeptidyl-peptidase; MCA, dipeptidyl-4-methycoumaryl-7-amide.

Growth retardation of Escherichia coli *expressing DPP7*

In previous studies, when the full-length forms of *P. gingivalis* DPPs were expressed as C-terminal hexa-His-tagged proteins, recombinant molecules were recovered as mature forms in *E. coli* cell lysates (26, 28, 33). Because of its broad substrate specificity, overexpressed DPP7 may be more harmful to the host than other DPPs, thus in the present study, we compared the growth rates of *E. coli* harboring a DPP4-expression plasmid, DPP5-expression plasmid, DPP7-expression plasmid, or DPP11-expression plasmid. When *E. coli* was cultured in Luria–Bertani broth containing 2% (w/v) glucose, a condition known to suppress expression, all cells grew in a regular manner for up to 8 h (Fig. 8*A*). In contrast, in the presence of IPTG, cells expressing DPP7 showed no growth, whereas the growth of bacteria expressing DPP5 was severely limited and that of those with DPP11 expression was partially retarded (Fig. 8*B*). DPP4-expressing cells grew similarly to those in the noninducing condition. These results indicated a wide difference in substrate preference among DPPs, that is, the preference of DPP4 and DPP11 was shown to be restricted, whereas DPP7 demonstrated a broad substrate specificity, followed by DPP5. Actually, we noticed a relatively poor recovery of recombinant DPP7 in the present *E. coli* expression system as compared with the other DPPs.

Discussion

It is disadvantageous for *P. gingivalis* if the bacterium cannot wholly convert nutritional peptides to dipeptides, taking into account its habitat in subgingival dental plaque along with a large number of bacterial competitors. Thus, observations that even the combination of substrate specificities of DPP4, DPP5, DPP7, and DPP11 do not fully cover dipeptidyl-MCA with P1-position Ser, Thr, Gln, Asn, Gly, and His highlight a long-standing issue (35). The present findings solved this problem and even showed degradation of gastrointestinal peptides by bacterial DPP7.

The P1 repertoires of *P. gingivalis* DPPs are summarized in Figure 9. The present study revealed a broad substrate preference of DPP7, from Glu (HI = −31) to Ala (HI = 41), together with authentic specificity for hydrophobic residues. Although DPP7 targeted P1 Lys and Glu under the experimental conditions, those residues could be primarily managed by Kgp and DPP11, respectively, in the bacterium. Hack *et al.* (36) reported that DPP7 from *Capnocytophaga canimorsus*, a human

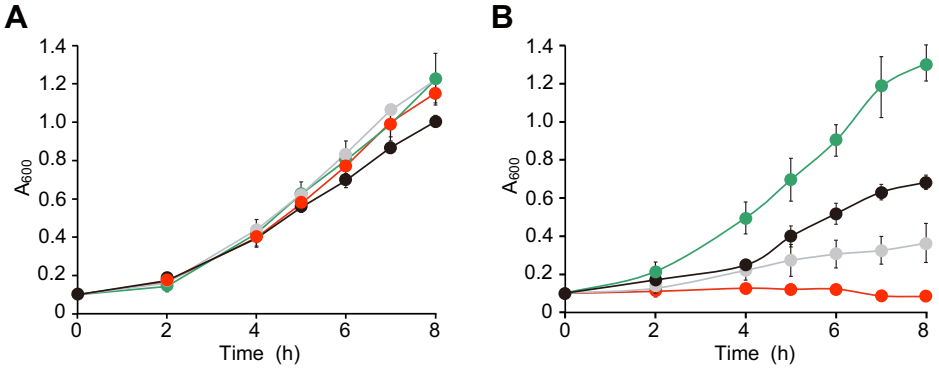

Figure 8. Growth of *Escherichia coli* XL-1 Blue harboring an expression plasmid of DPP. Overnight culture of *E. coli* was diluted to an absorbance of 0.1 at 600 nm in Luria–Bertani medium containing 75 µg/ml of ampicillin either with (*A*) 2% (w/v) glucose (noninducing condition) or (*B*) 0.2 mM IPTG (inducing condition). Bacterial cells were further cultured at 30 °C for 8 h, and an absorbance at 600 nm was monitored. *E. coli* harboring the plasmid encoding DPP7 (*red*), DPP4 (*green*), DPP5 (*gray*), or DPP11 (*black*). Data are means ± SD of three independent cultures. Typical data of three separate experiments are shown. DPP, dipeptidyl-peptidase; IPTG, isopropyl β-D-1-thiogalactopyranoside.

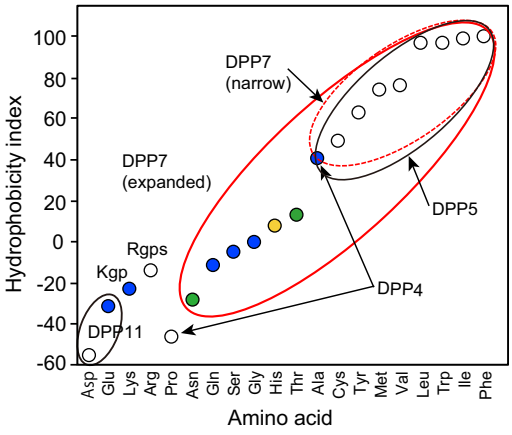

Figure 9. Repertoires of P1 amino acids covered by *Porphyromonas gingivalis* DPPs. The repertoires of P1 amino acids managed by DPP4, DPP5, DPP7, DPP11, Lys-gingipains (Kgp), and Arg-gingipains (Rgps) are indicated in connection with HI. Repertoires of DPP7 established in earlier studies (*narrow*) and the present study (*expanded*) are shown in *red broken and solid ellipses*, respectively. Acidic residues (Asp and Glu) are cleaved by DPP11 (*black ellipse*). The present study indicated that DPP7 cleaved P1-position Ala, Gly, Ser, Gln, Lys, and Glu (*blue*). Cleavages at Thr and Asn (*green*) were previously reported (36). The expanded specificity may cover His (*yellow*) (see the text). Glu and Lys are primarily managed by DPP11 and Lys-gingipain/Kgp, respectively, in *P. gingivalis*. DPP, dipeptidyl-peptidase; HI, hydrophobicity index.

pathogen associated with animal bites, degrades peptide bonds of coagulation factor X with P1-position Thr and Asn. In consideration of those and the present findings, we here propose that DPP7 covers P1-position residues from Asn (HI = −28) to Phe (HI = 100) (Fig. 9, expanded substrate specificity shown as *red-line ellipse*). Despite no known results regarding His, it is likely that DPP7 recognizes this residue with an HI value of 8. Thus, DPP7 with a broad substrate specificity seems to play a central role in dipeptide production in *P. gingivalis*, and the toxicity of recombinant DPP7 toward *E. coli* may reflect its broad substrate preference.

Intravenous administration of DPP7 in mice decreased serum levels of active GLP-1, suggesting that DPP7 can modulate blood glucose levels. DPP7 was also shown to hydrolyze insulin, though the degradation rate of insulin was significantly slower as compared with incretin peptides (Table 2). Thus, the effect of DPP7 on blood glucose levels seems to be mainly mediated by inactivation of incretins rather than degradation of insulin. Nevertheless, the fact that insulin can be a substrate of DPP7 is important, since insulin-degrading enzyme has been reported to cleave amyloid β and have a correlation with Alzheimer's disease (37). It is therefore considered imperative to search for bioactive peptides that serve as substrates for DPP7.

Bacteremia caused by oral bacteria occurs in association with daily activities such as food chewing and tooth brushing, as well as dental treatment, and the incidence, duration, and magnitude are shown to correlate with periodontal status (38, 39). Therefore, it is reasonable to speculate that DPP7 and DPP4 derived from *P. gingivalis* and other periodontopathic subgingival bacteria (40) when transferred into the bloodstream are unignorable factors that potentially link periodontal diseases with type 2 diabetes mellitus. Since both of those diseases develop over a long period, cumulative incidence and the high magnitude of periodontal bacteremia in individuals suffering from severe periodontal disease might cause an increase in blood glucose level as well as duration of hyperglycemia *via* degradation of incretins.

Clinical aspects of the present findings are important. DPP4 is expressed in both bacteria and humans, and DPP4 inhibitors could provide supplementary inhibition of bacterial DPP4 (26). In contrast, the distribution of DPP7 is limited in subgingival bacteria in the oral cavity (40) and gut anaerobic bacteria (33). Hence, development of a DPP7 inhibitor seems to be a convincing approach for systemic disorders related to periodontal diseases, as more than 47% of adults in the United States aged 30 years and older suffer from periodontal diseases (41). It is crucial to compare bacterial DPP7 activity in blood between healthy and diseased individuals in a future study.

Peptidyl-MCA and *p*-nitroanilide measurements are quantitative and convenient for determining substrate specificity and the catalytic parameters of proteases. However, these substrates have a disadvantage of not being able to evaluate the effects of prime-side residues. To overcome this issue, we developed a two-step reaction method using tripeptidyl-MCA and tetra-peptidyl-MCA coupled with appropriate exopeptidases. With use of that method, the present study is the first to demonstrate that P1′ and P2′ residues increase the turnover rate of DPP7 and DPP11 and that the effect was most significant for the substrate with a nonpreferable and nonrepulsive residue at the P1 position. We consider that enzymatic parameters of peptidases determined by this two-step reaction method are likely comparable to those for the bioactive polypeptides examined in the present study.

A possible conjecture is that elongation of the synthetic substrate moves the MCA moiety away from the cleavage site, thus canceling the unyielding structure of MCA. On the other hand, several of the findings indicated a positive effect in the prime-side region. Not only the P1′ residue but also the P2′ residue facilitated the enzymatic reaction, and second, the extent of enhancement was affected by the amino acid species at the P1′ position (Fig. 6). These results indicate that the activity of DPP7 was increased through interactions with prime-side residues.

It has been shown that a high k_{cat}/K_M ratio for substrates is mainly accomplished from an increase in k_{cat} rather than K_M in S1-family proteases, such as trypsin and pancreatic elastase (42). This event was also allocated to DPP7, since its highest k_{cat}/K_M ratio was shown to be mediated by the largest k_{cat} level among the dipeptidyl-MCAs tested (Table 2).

This study also revealed that a rise of k_{cat} by prime-side residues was common in S46 family peptidases. A preliminary search with glutamyl endopeptidase I/V8 protease/GluC (S1.269) from *Staphylococcus aureus* indicated that this peptidase is also enhanced by prime-side residues (T.K. Nemoto, unpublished observation). Accordingly, activity enhancement by prime-side residues is not a specific phenomenon seen only in the S46 family.

Banbula *et al.* (27) were the first to clone and characterize *P. gingivalis* DPP7. According to their report, DPP7 liberates N-terminal dipeptides from four synthetic oligopeptides with P1-position Ala (two cases), Ile, and Leu. However, they did not describe liberation of subsequent dipeptides, which is apparently incompatible with the present results. When we carefully checked their results, the P1-position residues of the subsequent dipeptide sequences are Gly (two cases), Glu, and Arg. The present study revealed that Gly and Glu in gastrointestinal peptides were slowly hydrolyzed, but Arg was not cleaved by DPP7 (Table 1). This may explain why sequential cleavages by DPP7 were not detected in the preceding study.

The 3D structure of the DPP7-family member DAPBII from *Pseudoxanthomonas mexicana* has been reported (43). Several inactive mutants were complexed with an octapeptide (DRVYIHPF). In an His86Ala mutant of DAPBII, clear electron density was observed from the third to seventh residue (VYIHP) of the octapeptide, corresponding to the P2-P1-P1′-P2′-P3′-position residues. Thus, the P3′ residue might be involved in enhancement of DPP7 activity. We previously reported that the 3D structure of DPP11 from *Porphyromonas endodontalis* was associated with the tetrapeptide LDVW (44). In the complex, the P1′-positon Val displayed a weakly defined electron density, with 40% of its solvent-accessible area buried by DPP11. These crystallographic observations are consistent with the present results demonstrating that prime-side residues contribute to the enzyme activities of S46-family DPP7 and DPP11.

An alignment search in substrate peptides for *P. gingivalis* and human DPP4 revealed that the substrates have a higher frequency of aliphatic/hydrophobic side chains (Val, Phe, and Ile) in the P1′ position (45). Examination of the 3D structure of human DPP4 complexed with the N-terminal decapeptide of neuropeptide Y indicated that P1′ and P2′ residues (Ser^3-Lys^4), as well as P1 and P2 residues (Tyr^1-Pro^2), are associated with DPP4 through nonspecific, that is, amino acid-independent interactions (46). Accordingly, the activity of S9 family peptidases could be enhanced by prime-side residues, though this was not seen in *P. gingivalis* DPP4 and DPP5 in the present study (Fig. 5). We suspect that enzymatic activities of S9 family members may be highly dependent on the nonprime-side region, then the effect of prime-side residues on such activity becomes buried.

In conclusion, this study presents two primary findings. First, DPP7 exhibits more potent activity and expanded substrate specificity than previously reported. The expanded activity by P1′ and P2′ residues was shown to occur *via* enhancement of k_{cat}. Second, the broad substrate preference of potent activity allows *P. gingivalis* DPP7 to degrade incretins and other bioactive peptides, which may be related to systemic disorders.

Experimental procedures

Materials

Restriction and DNA-modifying enzymes were purchased from Takara Bio and New England Biolabs. Quick *Taq* HS DyeMix came from Toyobo. Oligonucleotide primers were synthesized by FASMAC. Leupeptin, Gly-Pro-MCA, His-Ala-MCA, Lys-Ala-MCA, Phe-Met-MCA, [(2*S*, 3*S*)-3-carboxyoxirane-2-carbonyl]-L-leucine (4-guanidinobutyl) amide hemihydrate, GLP-1, GIP, glucagon, oxyntomodulin, and substance-P were purchased from Peptide Institute. Gly-Phe-MCA and Ser-Tyr-MCA were obtained from Bachem. Other substrates not commercially available, that is, His-Ala-MCA, Gly-Ala-MCA, Tyr-Ala-MCA, Phe-Leu-MCA, HAED-MCA, HAEG-MCA, HAEF-MCA, YAED-MCA, LDKA-MCA, TDKA-MCA, and HAEGTF-MCA, were synthesized by Scrum. CCL3 and CXCL6 were provided by GenScript Japan. Bovine insulin, tosyl-L-lysyl-chloromethane hydrochloride, aprotinin, sitagliptin phosphate monohydrate, 3,4-dichloroisocoumarin, 4-(2-aminoethyl) benzenesulfonyl fluoride hydrochloride, and α-cyano-4-hydroxycinnamic acid were obtained from Sigma–Aldrich. Isoleucine thiazolidide hemifumarate (P32/98) was from FOCUS Biomolecules.

Bacterial strains and culture conditions

P. gingivalis American Type Culture Collection 33277 derivatives NDP200 (Δ*dpp4*), NDP400 (Δ*dpp7*), NDP210 (Δ*dpp4*–Δ*dpp7*), and NDP211 (Δ*dpp4*–Δ*dpp5*–Δ*dpp7*) have been previously described (26). NDP110 (Δ*dpp4*–Δ*dpp5*) was prepared from NDP100 (*dpp4*::*erm*) by introducing the *cepA* fragment to the *dpp5* gene, according to a reported method (26). *P. gingivalis* was grown anaerobically at 37 °C (80% N_2, 10% CO_2, and 10% H_2) in anaerobic bacterial culture medium broth (EIKEN Chemical) supplemented with 0.5 μg ml^{-1} of menadione. Appropriate antibiotics (ampicillin, erythromycin, and tetracycline) were added for cultures of *dpp*-deleted strains. *P. gingivalis* cells were harvested in the early stationary phase and washed with ice-cold PBS, pH 7.3, then suspended in PBS for adjustment to 0.2 at an absorbance at 600 nm.

Expression and purification of recombinant DPPs

Expression plasmids for *P. gingivalis* DPP4 (33), DPP5 (26), DPP7 (33), and DPP11 (28) and for *P. intermedia* and *T. forsythia* DipA (34) with a C-terminal hexa-His-tag have been previously reported. *E. coli* XL-1 Blue cells carrying an expression plasmid were cultured in Luria–Bertani broth supplemented with 75 μg ml^{-1} ampicillin at 37 °C overnight. After addition of two volumes of fresh media, recombinant proteins were induced with 0.2 mM IPTG at 30 °C for 4 h, then purified from the bacterial cell lysate using TALON affinity chromatography, as previously described (28).

MALDI-TOF MS

P. gingivalis cell suspensions (8 μl, absorbance at 600 nm = 2.0) were preincubated in 80 μl of 50 mM sodium phosphate buffer, pH 7.5, containing 5 mM EDTA, 0.5 mM tosyl-L-lysyl-chloromethane hydrochloride, and 30 μM [(2*S*, 3*S*)-3-carboxyoxirane-2-carbonyl]-L-leucine (4-guanidinobutyl) amide hemihydrate for 10 min at 0 °C to inhibit gingipain activities. A reaction was started by adding 20 μl of GLP-1 or GIP (20 μM) at 37 °C, and then MS analysis was performed as

previously reported (12, 28). The reaction was stopped at the appropriate time by transferring an aliquot (12 μl) of the reaction mixture to a new tube containing trifluoroacetic acid (0.1%). Hydrolyzed products were adsorbed to a Millipore ZipTip-C18 by 10 times pipetting, washed four times with 10 μl of 0.1% trifluoroacetic acid, and eluted by 10 times pipetting with 10 μl of 50% acetonitrile containing 5 mg ml^{-1} of α-cyano-4-hydroxycinnamic acid. Eluted samples (0.5 μl) were spotted on a target plate and dried. Hydrolysis of 20 μM peptide substrates was also performed with aliquots of DPPs (1–100 ng). The molecular mass of each product was determined by MS using Voyager DE-Pro (Applied Biosystems) and Ultraflex III (Bruker) devices. The molecular weights of all peptide fragments were calculated with the ProtParam (https://web.expasy.org/protparam), and $t_{1/2}$ was determined from the decrease in ratios of the remaining intact molecule per the sum of all degraded peptides.

Peptidase activity measurement

The reaction was started by addition of recombinant DPPs (0.5–100 ng) or a bacterial cell suspension (1–5 μl) in a reaction mixture (200 μl) composed of 50 mM sodium phosphate (pH 7.5), 5 mM EDTA, and 20 μM peptidyl-MCA. All reactions were performed at 37 °C. After 30 min, fluorescence intensity was measured with excitation at 380 nm and emission at 460 nm. Decomposition of the substrate up to 10% could be determined as a first-order reaction. DPP4, DPP5, DPP7, and DPP11 activities were generally determined using a DPP-specific substrate, Gly-Pro-MCA (24), Gly-Phe-MCA (26), Phe-Met-MCA (47), and Leu-Asp-MCA (28), respectively. Other synthetic substrates, including His-Ala-MCA, HAR-MCA, HAL-MCA, HAEG-MCA, HAED-MCA, HAEF-MCA, HALD-MCA, and HAEGTF-MCA, mimic the N-terminal sequence of human GLP-1 (identical residues to GLP-1 sequence are underlined), whereas Tyr-Ala-MCA and YAED-MCA partially mimic the N-terminal sequence of human GIP (amino acids: 52–93) (identical residues to GLP-1 sequence are underlined). To evaluate the roles of the P1′ and P2′ residues, we used tetrapeptidyl-MCA, that is, HAED-MCA, YAED-MCA, HALD-MCA, LDKA-MCA, and TDKA-MCA, and tripeptidyl-MCA, that is, HAR-MCA and HAL-MCA, as substrates for the two-step reaction. Tetrapeptidyl-MCA and tripeptidyl-MCA were incubated with the examined DPP in the absence or presence of an excess amount of appropriate second DPP or DipA, respectively, which resulted in release of 7-amino-4-methylcoumarin with fluorescence. Conditions for two-step reactions were employed for those of the first examined DPP, as hydrolysis of tetrapeptidyl-MCA and tripeptidyl-MCA is tightly dependent on the activity of the first DPP (Figs. 5–7).

Glucose tolerance test in mice

C57BL/6N female mice were purchased from Charles River Laboratory. All animal experiments were approved by the Animal Ethics Committee of Nagasaki University (no.: 0911170797) and performed as previously described (12). Briefly, purified recombinant DPP7 was dialyzed against PBS at 4 °C and then sterilized with a membrane filter (pore size = 0.22 μm). DPP7 activity in each fraction was determined using Phe-Met-MCA. After fasting for 15 h, an appropriate amount (1 U 100 μl^{-1} PBS) of DPP7 was injected *via* the tail vein into 11-week-old to 13-week-old mice. An identical volume of sterilized PBS was injected into the control group. Two minutes after injection, a glucose solution (3 mg g^{-1} body weight) was orally administrated, and blood glucose level was measured using an OneTouch UltraVue device (Johnson & Johnson). For measurements of GLP-1 (amino acids: 7–37) (active form) and insulin, blood specimens were obtained from the heart at 15 min after glucose administration and gently mixed with peptidase inhibitors composed of 0.5 KIU μl^{-1} aprotinin, 2 μM P32/98, 1 mM 3,4-dichloroisocoumarin, 2 μg μl^{-1} 4-(2-aminoethyl) benzenesulfonyl fluoride hydrochloride, and 2 mM EDTA. Plasma was collected by centrifugation at 1200*g* at 4 °C and stored immediately at −80 °C until use. Concentrations of GLP-1 (amino acids: 7–37) were measured using an ELISA kit from Shibayagi, whereas those of insulin were determined with an Ultrasensitive Mouse/Rat Insulin ELISA kit (Morinaga Institute of Biological Science), according to the manufacturer's protocols. Data are presented as the mean ± SD and were analyzed using the GraphPad Prism software package (GraphPad Software, Inc). Statistical significance was determined for parametric data by an unpaired Student's *t* test with Welch's correction. A p value of <0.05 was considered to indicate statistical significance.

Protein concentration

The concentrations of purified proteins were determined using Coomassie brilliant blue dye (Bio-Rad).

Data availability

All data are contained within the article.

Supporting information—This article contains supporting information.

Author contributions—Y. O.-N. and T. K. N. conceptualization; Y. S., T. O., M. T. S., M. N., and M. S. methodology; T. O. resources; Y. O.-N. and T. K. N. writing–review & editing; Y. O.-N. visualization; T. K. N. supervision; Y. O.-N. and T. K. N. funding acquisition.

Funding and additional information—This study was supported by the Japan Society for the Promotion of Science KAKENHI grants (JP19K10045 to T. K. N., JP19K10071 to Y. O.-N., and JP19K19005 to M. N.) and a grant from the Kyushu Dental Association (to T. K. N.).

Conflict of interest—The authors declare that they have no conflicts of interest with the contents of this article.

Abbreviations—The abbreviations used are: CCL3, chemokine (C–C motif) ligand 3; CXCL6, chemokine (C–X–C motif) ligand 6; DipA, dipeptidase A; DPP, dipeptidyl-peptidase; GIP, gastric inhibitory

polypeptide; GLP-1, glucagon-like peptide-1; HI, hydrophobicity index; MCA, dipeptidyl-4-methycoumaryl-7-amide; MS, mass spectrometry.

References

1. Socransky, S. S., and Haffajee, A. D. (2002) Periodontal microbial ecology. *Periodontol. 2000* **38**, 135–187
2. Holt, S. C., and Ebersole, J. L. (2005) *Porphyromonas gingivalis, Treponema denticola*, and *Tannerella forsythia*: The 'red complex', a prototype polybacterial pathogenic consortium in periodontitis. *Periodontol. 2000* **38**, 72–122
3. Grossi, S. G., and Genco, R. J. (1998) Periodontal disease and diabetes mellitus: A two-way relationship. *Ann. Periodontol.* **3**, 51–61
4. Lalla, E., and Papapanou, P. N. (2011) Diabetes mellitus and periodontitis: A tale of two common interrelated diseases. *Nat. Rev. Endocrinol.* **7**, 738–748
5. Preshaw, P. M., Alba, A. L., Herrera, D., Jepsen, S., Konstantinidis, A., Makrilakis, K., and Taylor, R. (2012) Periodontitis and diabetes: A two-way relationship. *Diabetologia* **55**, 21–31
6. Genco, R. J., and VanDyke, T. E. (2010) Prevention: Reducing the risk of CVD in patients with periodontitis. *Nat. Rev. Cardiol.* **7**, 479–480
7. Tabeta, K., Yoshie, H., and Yamazaki, K. (2014) Current evidence and biological plausibility linking periodontitis to atherosclerotic cardiovascular disease. *Jpn. Dent. Sci. Rev.* **50**, 55–62
8. Kshirsagar, A. V., Offenbacher, S., Moss, K. L., Barros, S. P., and Beck, J. D. (2007) Antibodies to periodontal organisms are associated with decreased kidney function: The dental atherosclerosis risk in communities study. *Blood Purif.* **25**, 125–132
9. Detert, J., Pischon, N., Burmester, G. R., and Buttgereit, F. (2010) The association between rheumatoid arthritis and periodontal disease. *Arthritis Res. Ther.* **12**, 218
10. Teixeira, F. B., Saito, M. T., Matheus, F. C., Prediger, R. D., Yamada, E. S., Maia, C. S. F., and Lima, R. R. (2017) Periodontitis and Alzheimer's disease: A possible comorbidity between oral 495 chronic inflammatory condition and neuroinflammation. *Front. Aging Neurosci.* **9**, 327
11. Genco, R. J., Grossi, S. G., Ho, A., Nishimura, F., and Murayama, Y. (2005) A proposed model linking inflammation to obesity, diabetes, and periodontal infections. *J. Periodontol.* **76**, 2075–2084
12. Ohara-Nemoto, Y., Nakasato, M., Shimoyama, Y., Baba, T. T., Kobayakawa, T., Ono, T., Yaegashi, T., Kimura, S., and Nemoto, T. K. (2017) Degradation of incretins and modulation of blood glucose levels by periodontopathic bacterial dipeptidyl peptidase 4. *Infect. Immun.* **85**, e00277-17
13. Tang-Larsen, J., Claesson, R., Edlund, M. B., and Carlsson, J. (1995) Competition for peptides and amino acids among periodontal bacteria. *J. Periodontal Res.* **30**, 390–395
14. Takahashi, N., and Sato, T. (2001) Preferential utilization of dipeptides by *Porphyromonas gingivalis*. *J. Dent. Res.* **80**, 1425–1429
15. Takahashi, N., and Sato, T. (2002) Dipeptide utilization by the periodontal pathogens *Porphyromonas gingivalis, Prevotella intermedia, Prevotella nigrescens* and *Fusobacterium nucleatum*. *Oral Microbiol. Immunol.* **17**, 50–54
16. Ohara-Nemoto, Y., Sarwar, M. T., Shimoyama, Y., Kobayakawa, T., and Nemoto, T. K. (2020) Predominant dipeptide incorporation in *Porphyromonas gingivalis* mediated *via* a proton-dependent oligopeptides transporter (Pot). *FEMS Microbiol. Lett.* **367**, 1–8
17. Suido, H., Nakamura, M., Mashimo, P. A., Zambon, J. J., and Genco, R. J. (1986) Arylaminopeptidase activities of oral bacteria. *J. Dent. Res.* **65**, 1335–1340
18. Nemoto, T. K., Ohara-Nemoto, Y., Bezerra, G. A., Shimoyama, Y., and Kimura, S. (2016) A *Porphyromonas gingivalis* periplasmic novel exopeptidase, acylpeptidyl oligopeptidase, releases N-acylated di- and tripeptides from oligopeptides. *J. Biol. Chem.* **291**, 5913–5925
19. Banbula, A., Mak, P., Bugno, M., Silberring, J., Dubin, A., Nelson, D., Travis, J., and Potempa, J. (1999) Prolyl tripeptidyl peptidase from *Porphyromonas gingivalis*. A novel enzyme with possible pathological implications for the development of periodontitis. *J. Biol. Chem.* **274**, 9246–9252
20. Nemoto, T. K., and Ohara-Nemoto, Y. (2020) Dipeptidyl-peptidases: Key enzymes producing entry forms of extracellular proteins in asaccharolytic periodontopathic bacterium *Porphyromonas gingivalis*. *Mol. Oral Microbiol.* **36**, 145–156
21. Rawlings, N. D., Barrett, A. J., Thomas, P. D., Huang, X., Bateman, A., and Finn, R. D. (2018) The MEROPS database of proteolytic enzymes, their substrates and inhibitors in 2017 and a comparison with peptidases in the PANTHER database. *Nucleic Acids Res.* **46**, D624–D632
22. Mentlein, R. (1988) Proline residues in the maturation and degradation of peptide hormones and neuropeptides. *FEBS Lett.* **234**, 251–256
23. Keane, F. M., Nadvi, N. A., Yao, E.-W., and Gorrell, M. D. (2011) Neuropeptide Y, B-type natriuretic peptide, substance P and peptide YY are novel substrates of fibroblast activation protein-α. *FEBS J.* **278**, 1316–1332
24. Banbula, A., Bugno, M., Goldstein, J., Yen, J., Nelson, D., Travis, J., and Potempa, J. (2000) Emerging family of proline-specific peptidases of Porphyromonas gingivalis: Purification and characterization of serine dipeptidyl peptidase, a structural and functional homologue of mammalian prolyl dipeptidyl peptidase IV. *Infect. Immun.* **68**, 1176–1182
25. Beauvais, A., Monod, M., Debeaupuis, J. P., Diaquin, M., Kobayashi, H., and Latgé, J. P. (1997) Biochemical and antigenic characterization of a new dipeptidyl-peptidase isolated from *Aspergillus fumigatus*. *J. Biol. Chem.* **272**, 6238–6244
26. Ohara-Nemoto, Y., Rouf, S. M. A., Naito, M., Yanase, A., Tetsuo, F., Ono, T., Kobayakawa, T., Shimoyama, Y., Kimura, S., Nakayama, K., Saiki, K., Konishi, K., and Nemoto, T. K. (2014) Identification and characterization of prokaryotic dipeptidyl-peptidase 5 from *Porphyromonas gingivalis*. *J. Biol. Chem.* **289**, 5436–5448
27. Banbula, A., Yen, J., Oleksy, A., Mak, P., Bugno, M., Travis, J., and Potempa, J. (2001) *Porphyromonas gingivalis* DPP-7 represents a novel type of dipeptidylpeptidase. *J. Biol. Chem.* **276**, 6299–62305
28. Ohara-Nemoto, Y., Shimoyama, Y., Kimura, S., Kon, A., Haraga, H., Ono, T., and Nemoto, T. K. (2011) Asp- and Glu-specific novel dipeptidyl peptidase 11 of Porphyromonas gingivalis ensures utilization of proteinaceous energy sources. *J. Biol. Chem.* **286**, 38115–38127
29. Rouf, S. M. A., Ohara-Nemoto, Y., Ono, T., Shimoyama, Y., Kimura, S., and Nemoto, T. K. (2013) Phenylalanine664 of dipeptidyl peptidase (DPP) 7 and phenylalanine671 of DPP11 mediate preference for P2-position hydrophobic residues of a substrate. *FEBS Open Bio* **3**, 177–181
30. Mentlein, R., Gallwitz, B., and Schmidt, W. E. (1993) Dipeptidyl-peptidase IV hydrolyses gastric inhibitory polypeptide, glucagon-like peptide-1(7-36)amide, peptide histidine methionine and is responsible for their degradation in human serum. *Eur. J. Biochem.* **214**, 829–835
31. Gallwitz, B. (2019) Clinical use of DPP-4 inhibitors. *Front. Endocrinol.* **10**, 389
32. Monera, O. D., Sereda, T. J., Zhou, N. E., Kay, C. M., and Hodges, R. S. (1995) Relationship of sidechain hydrophobicity and a-helical propensity on the stability of the single-stranded amphipathic α-helix. *J. Pept. Sci.* **1**, 319–329
33. Rouf, S. M. A., Ohara-Nemoto, Y., Hoshino, T., Fujiwara, T., Ono, T., and Nemoto, T. K. (2013) Discrimination based on Gly and Arg/Ser at position 673 between dipeptidyl-peptidase (DPP) 7 and DPP11, widely distributed DPPs in pathogenic and environmental Gram-negative bacteria. *Biochimie* **95**, 824–832
34. Sarwar, M. T., Ohara-Nemoto, Y., Kobayakawa, T., Naito, M., and Nemoto, T. K. (2020) Characterization of substrate specificity and novel autoprocessing mechanism of dipeptidase A from *Prevotella intermedia*. *Biol. Chem.* **401**, 629–642
35. Nemoto, T. K., and Ohara-Nemoto, Y. (2016) Exopeptidases and gingipains in *Porphyromonas gingivalis* as prerequisites for its amino acid metabolism. *Jpn. Dent. Sci. Rev.* **52**, 22–29
36. Hack, K., Renzi, F., Hess, E., Lauber, F., Douxfils, J., Dogné, J. M., and Cornelis, G. R. (2017) Inactivation of human coagulation factor X by a protease of the pathogen *Capnocytophaga canimorsus*. *J. Thromb. Haemost.* **15**, 487–499

37. Kurochkin, I. V., and Goto, S. (1994) Alzheimer's β-amyloid peptide specifically interacts with and is degraded by insulin degrading enzyme. *FEBS Lett.* **345**, 33–37
38. Forner, L., Larsen, T., Kilian, M., and Holmstrup, P. (2006) Incidence of bacteremia after chewing, tooth brushing and scaling in individuals with periodontal inflammation. *J. Clin. Periodontol.* **33**, 401–407
39. Lockhart, P. B., Brennan, M. T., Sasser, H. C., Fox, P. C., Paster, B. J., and Bahrani-Mougeot, F. K. (2008) Bacteremia associated with tooth brushing and dental extraction. *Circulation* **117**, 3118–3125
40. Ohara-Nemoto, Y., Shimoyama, Y., Nakasato, M., Nishimata, H., Ishikawa, T., Sasaki, M., Kimura, S., and Nemoto, T. K. (2018) Distribution of dipeptidyl peptidase (DPP)4, DPP5, DPP7 and DPP11 in human oral microbiota-potent biomarkers indicating presence of periodontopathic bacteria. *FEMS Microbiol. Lett.* **365**. https://doi.org/10.1093/femsle/fny221
41. Eke, P. I., Dye, B. A., Wei, L., Thornton-Evans, G. O., and Genco, R. J. (2021) Prevalence of periodontitis in adults in the United States: 2009 and 2010. *J. Dent. Res.* **91**, 914–920
42. Hedstrom, L. (2002) Serine protease mechanism and specificity. *Chem. Rev.* **102**, 4501–4524
43. Sakamoto, Y., Suzuki, Y., Iizuka, I., Iizuka, I., Tateoka, C., Roppongi, S., Fujimoto, M., Inaka, K., Tanaka, H., Masaki, M., Ohta, K., Okada, H., Nonaka, T., Morikawa, Y., Nakamura, K. T., *et al.* (2014) S46 peptidases are the first exopeptidases to be members of clan PA. *Sci. Rep.* **15**, 4977
44. Bezerra, G. A., Ohara-Nemoto, Y., Cornaciu, I., Fedosyuk, S., Hoffmann, G., Round, A., Márquez, J. A., Nemoto, T. K., and Djinović-Carugo, K. (2017) Bacterial protease uses distinct thermodynamic signatures for substrate recognition. *Sci. Rep.* **7**, 2848
45. Rea, D., Van Elzen, R., De Winter, H., Van Goethem, S., Landuyt, B., Luyten, W., Schoofs, L., Van Der Veken, P., Augustyns, K., De Meester, I., Fülöp, V., and Lambeir, A. M. (2017) Crystal structure of *Porphyromonas gingivalis* dipeptidyl peptidase 4 and structure-activity relationships based on inhibitor profiling. *Eur. J. Med. Chem.* **139**, 482–491
46. Aertgeerts, K., Ye, S., Tennant, M. G., Kraus, M. L., Rogers, J., Sang, B. C., Skene, R. J., Webb, D. R., and Prasad, G. S. (2004) Crystal structure of human dipeptidyl peptidase IV in complex with a decapeptide reveals details on substrate specificity and tetrahedral intermediate formation. *Protein Sci.* **13**, 412–421
47. Nemoto, T. K., Ono, T., and Ohara-Nemoto, Y. (2018) Establishment of potent and specific synthetic substrate for dipeptidyl-peptidase 7. *Anal. Biochem.* **548**, 78–81